Analysis of mutations at positions 115 and 116 in the dNTP binding site of HIV-1 reverse transcriptase

Paul L. Boyer*†, Stefan G. Sarafianos‡, Edward Arnold‡, and Stephen H. Hughes*†§

*Advanced BioScience Laboratories-Basic Research Program, National Cancer Institute-Frederick Cancer Research and Development Center, P.O. Box B, Frederick, MD 21702-1201; and ‡Center for Advanced Biotechnology and Medicine and Rutgers University Chemistry Department, 679 Hoes Lane, Piscataway, NJ 08854-5638

Communicated by George F. Vande Woude, Van Andel Research Institute, Grand Rapids, MI, December 31, 1999 (received for review April 25, 1999)

We have examined amino acid substitutions at residues 115 and 116 in the reverse transcriptase (RT) of HIV-1. A number of properties were examined, including polymerization and processivity on both DNA and RNA templates, strand displacement, ribonucleotide misincorporation, and resistance to nucleoside analogs. The RT variants Tyr-115–Phe and Phe-116–Tyr are similar to wild-type HIV-1 RT in most, but not all, respects. In contrast, the RT variant Tyr-115–Val is significantly impaired in polymerase activity compared with wild-type RT; however, Tyr-115–Val is able to incorporate ribonucleotides as well as deoxyribonucleotides during polymerization and is resistant to a variety of nucleoside analogs.

The reverse transcriptase (RT) of HIV-1 is essential for the replication of the virus (for a review, see ref. 1) and is an important target for antiviral therapy. Two major classes of RT inhibitors, nucleoside analogs and nonnucleoside inhibitors, have been discovered. However, mutations within RT engender resistance to both classes of inhibitors (for reviews, see refs. 2–4). To understand in greater detail how HIV-1 RT is able to mutate to render nucleoside analogs less effective, the nucleotide binding site at the polymerase active site must be studied in greater detail.

Based on the available crystal structures of Moloney murine leukemia virus (MMLV) RT and HIV-1 RT, models have been developed for nucleotide binding sites of these two related enzymes. In the available models (5), the amino acids Phe-155 (MMLV RT) and Tyr-115 (HIV-1 RT) interact with the deoxyribose of the incoming dNTP. The structure of a ternary complex of HIV-1 RT, a double-strand DNA, and a bound dTTP now has been determined (6) and shows that, as predicted (5), Tyr-115 interacts directly with the deoxyribose of the incoming triphosphate.

In analyzing mutations at Tyr-115, several groups have found that the only amino acid substitution that has little deleterious effect on the enzyme is Tyr-115–Phe (7–14). Substitution of Tyr-115 with polar amino acids is extremely deleterious (9–13) whereas substitution with hydrophobic amino acids usually has an intermediate effect (7, 8, 11, 12, 14). Recently, the Tyr-115–Phe mutation, along with the mutations Lys-65–Arg, Leu-74–Val, and Met-184–Val, has been detected in HIV-1 RTs resistant to the carbocyclic nucleoside analog 1592U89 (abacavir) (15, 16). The effects of amino acid substitutions at residue 116 have been less well characterized (7, 8), although the amino acid substitution Phe-116–Tyr is one of the mutations present in an RT variant resistant to multiple dideoxynucleotides (17–19). In this study, we have analyzed the effects of mutations Tyr-115–Phe, Tyr-115–Val, and Phe-116–Tyr in the nucleotide-binding pocket on the activity of HIV-1 RT.

Some of the substitutions we have chosen to make in HIV-1 RT represent amino acids found at the equivalent positions in other viral polymerases. As has already been mentioned, there is a phenylalanine in MMLV RT at the position equivalent to position 115 of HIV-1 RT (5), and a tyrosine in hepatitis B RT at the position equivalent to position 116 of HIV-1 RT (20). We also wanted to compare the effects of introducing valine at position 115 of HIV-1 RT with the MMLV RT mutant with valine at position 155 (21, 22).

Materials and Methods

Preparation of p66/p51 Heterodimers. *Bsp*MI cassette mutagenesis was used to introduce mutations into the p66 coding region (7, 23). The DNA segments encoding the "His-tagged" RT variants were cloned into the vector S-D prot, and the clones were then introduced into the *Escherichia coli* strain BL21 (DE3) pLysE (24). The resulting heterodimers were purified by metal chelation chromatography (24).

Polymerase and Inhibitor Assays. Wild-type RT and the variant RTs were analyzed for polymerase activity by using a variety of different template-primer substrates (Fig. 1). As described (26), we constructed a series of plasmids containing the polypurine tract (PPT, 5′-AAAAGAAAAGGGGGGGGA-3′), U3, R, U5, and the primer binding site (PBS, 5′-GTCCCTGTTCGGGCGCCA-3′) from the proviral clone pNL 4–3 (25) in the vectors Litmus 28 and Litmus 29 (Not).

For each enzyme sample to be assayed, 0.5 μg of single-strand DNA and 0.1 μl of 10 OD_{260}/ml oligonucleotide were hybridized. The mixture was adjusted to contain 25 mM Tris·Cl (pH 8.0), 75 mM KCl, 8.0 mM $MgCl_2$, 2 mM DTT, 1 μg/ml acetylated BSA, 10 mM CHAPS (3-[(3-cholamidopropyl)dimethylammonio]-1-propanesulfonate), 10 μM each of dATP and dTTP, 5 μM each of dGTP and dCTP, and 0.5 μl each of [α^{32}P]dGTP and [α^{32}P]dCTP in a final volume of 100 μl. The reaction was initiated by the addition of 0.1 μg of enzyme and was allowed to proceed for 1 h. The reactions were terminated by the addition of 10 μl of 10 mg/ml sheared, denatured salmon sperm DNA, and 3 ml of ice-cold 100% trichloroacetic acid (TCA). The precipitate was collected on Whatman GF/C glass filters and counted.

The RNA-dependent DNA-dependent polymerase (RDDP) assays used four template-primer combinations: (*i*) poly(rC)·oligo(dG) obtained from Amersham Pharmacia; (*ii*) poly(rA)·oligo(dT) obtained from Amersham Pharmacia; (*iii*) PPT-PBS antisense RNA hybridized to the PPT DNA oligonucleotide; and (*iv*) PPT-PBS sense RNA hybridized to the PBS DNA oligonucleotide. The last two RDDP assays are similar to the assays described previously (23) except that RNase-free reagents and 1 unit/μl RNase inhibitor (Ambion) were used.

Antisense RNA was generated from the *Spe*I-linearized plasmid PPT-PBS(T_n) by using the T7 MEGAscript kit and protocol (Ambion) as described (26); sense RNA was generated by using the *Not*I-linearized plasmid PPT-PBS(A_n). The full-length RNAs generated from these plasmids have poly(A) tails and were purified by using the PolyAT tract system (Promega).

Abbreviations: RT, reverse transcriptase; MMLV, Moloney murine leukemia virus; DDDP, DNA-dependent DNA polymerase; RDDP, RNA-dependent DNA polymerase; PPT, polypurine tract; PBS, primer binding site.

†Present address: HIV Drug Resistance Program, P.O. Box B, Building 539, Room 130A, National Cancer Institute-Frederick Cancer Research and Development Center, Frederick, MD 21702-1201.

§To whom reprint requests should be addressed.

The publication costs of this article were defrayed in part by page charge payment. This article must therefore be hereby marked "*advertisement*" in accordance with 18 U.S.C. §1734 solely to indicate this fact.

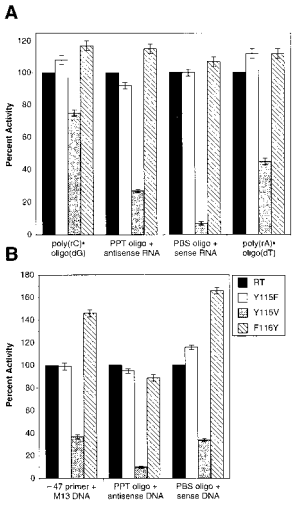

Fig. 1. Polymerase activity of the RT variants relative to wild-type RT. The level of radioactivity incorporated by wild-type RT represents 100% activity and the level of radioactivity incorporated by the RT variants is normalized to this value. The template primers used are described in *Materials and Methods*. (*A*) RDDP activities. (*B*) DDDP activities.

The inhibition of wild-type RT and the RT variants by the nucleoside analogs ddITP and ddGTP was assayed by using poly(rC)·oligo(dG) as the template-primer whereas the nucleoside analogs 3′-azido-3′-deoxythymidine 5′triphosphate (AZTTP) (Moravek Biochemicals, Brea, CA) and ddTTP were tested by using the template-primer poly(rA)·oligo(dT). Inhibition by (−)-β-L-2′,3′-dideoxy-3′-thiacytidine triphosphate (3TCTP) (Moravek Biochemicals) was assayed by using single-strand M13mp18 DNA (New England Biolabs) hybridized to the sequencing primer −47 (New England Biolabs).

Processivity and Strand-Displacement Assays. The processivity assay was done as described (27, 28). For the strand displacement assay, an end-labeled PBS DNA oligonucleotide was hybridized to single-strand PPT-PBS sense DNA generated from PPT-PBS L-28 along with a 10-fold excess of four unlabeled DNA oligonucleotides. There was a 10-nt gap between the 3′ end of the labeled PBS oligonucleotide and the 5′ end of the first unlabeled DNA oligonucleotide; the four unlabeled DNA oligonucleotides hybridize to regions of the HIV-1 long terminal repeat upstream of the PBS region separated by 3-nt gaps.

The RT reaction conditions were similar to those described above, except that the buffer conditions included either 75 mM or 35 mM KCl and that mixture was incubated at 37°C for 30 min. The reactions were halted by extraction with phenol/chloroform and the nucleic acid was precipitated with isopropanol, the sample was resuspended in 10 μl of loading dye, and 4 μl was loaded on a 6% sequencing gel. After electrophoresis, the gel was exposed to x-ray film.

UTP Misincorporation. The UTP misincorporation assay was similar to the DNA-dependent DNA polymerase (DDDP) assays described above, except that the reaction conditions included 10 μM each of dATP, dGTP, and dCTP, 1 μM dTTP, and 2 μl of 800 Ci/mmol [α^{22}P]UTP (1 μM final concentration). After a 30-min incubation at 37°C, the reaction mixture was passed through Sephacryl S-200-h, extracted with phenol/chloroform, and precipitated with isopropanol. The sample was resuspended in 10 μl of loading dye and 4 μl was loaded on a 6% sequencing gel. After electrophoresis, the gel was exposed to x-ray film.

dGTP and GTP Kinetics. The dGTP kinetic assay was done as described (26, 28) except that 20 μl of 1.0 mM dGTP solution was added to 177 μl of ddH_2O and 3 μl of 800 Ci/mmol [α^{32}P]dGTP to make a final concentration of 100 μM. The GTP kinetic assay was done in a similar manner except that radioactive 100 μM GTP mixture was made by mixing 20 μl of 1 mM GTP with 170 μl of ddH_2O and 10 μl of 3,000 Ci/mmol [α^{32}P]GTP. The reaction time also was increased from 10 min to 30 min because GTP is incorporated less efficiently than dGTP.

Results

Polymerase Assays. In the RDDP assay, RT variants Tyr-115–Phe and Phe-116–Tyr had RDDP activity slightly higher than that of wild-type RT whereas the RDDP activity of Tyr-115–Val was approximately 75% the level of wild-type RT (Fig. 1*A*). These results are in agreement with the results we obtained with p66 homodimers (7, 8). RDDP activity also was measured with a PPT DNA oligonucleotide hybridized to antisense RNA and with a PBS DNA oligonucleotide hybridized to sense RNA. As shown in Fig. 1*A*, the RT variants Tyr-115–Phe and Phe-116–Tyr had activity levels with these substrates, relative to wild-type HIV-1 RT, that were similar to their relative activity with poly(rC)·oligo(dG). However, Tyr-115–Val had a relative RDDP activity with the HIV-1 RNAs (both sense and antisense) that was significantly lower than the relative RDDP activity obtained with poly(rC)·oligo(dG). One possible explanation for this discrepancy is that Tyr-115–Val is able to use homopolymeric templates more efficiently than heteropolymeric templates. We tested this possibility by using another homopolymeric template: poly(rA)·oligo(dT). With poly(rA)·oligo(dT), the RT variants Tyr-115–Phe and Phe-116–Tyr had relative RDDP activities similar to the RDDP activity obtained with other substrates (Fig. 1*A*). Although Tyr-115–Val had a higher relative RDDP activity with poly(rA)·oligo(dT) than with either the sense or the antisense HIV-1 RNA templates, the relative RDDP activity was still significantly lower than that measured with poly(rC)·oligo(dG) (Fig. 1*A*).

Another possible explanation is that Tyr-115–Val might have a lower fidelity than wild-type RT and occasionally might incorporate an incorrect dNTP into the growing primer strand while using the heteropolymeric template. Such a misincorporation might cause the enzyme to stall at the misincorporated base. Only one nucleotide (dGTP) is present when poly(rC)·oligo(dG) is the template primer, so there would be neither misincorporation nor stalling. To test this possibility, we repeated the assay with poly(rC)·oligo(dG) except with equal amounts of all four dNTPs in the reaction mixture. The level of radioactive dGTP incorporated into poly(rC)·oligo(dG) remained the same whether or not the other dNTPs were present (data not shown), suggesting that misincorporation is not responsible for the differences in the relative RDDP activity obtained with poly(rC)·oligo(dG) and the other substrates.

The DDDP activity of the RT variant Tyr-115–Phe was similar to that of wild-type RT for all three substrates (Fig. 1*B*), whereas Phe-116–Tyr had relative DDDP activity levels that were higher than wild-type RT with two of the substrates (Fig. 1*B*). Tyr-115–Val was significantly impaired with all of the DDDP substrates when compared with wild-type RT (Fig. 1*B*).

Processivity. The results of the processivity assays with the PBS oligonucleotide and a sense HIV-1 DNA substrate are shown in Fig. 2*A*. The RT variant Tyr-115–Phe had the same relative processivity as wild-type RT whereas Phe-116–Tyr was more processive and Tyr-115–Val was significantly less processive relative to wild-type RT. In the RNA genome of HIV-1, there are two well-characterized secondary structures located in the R-U5 region: the Tar element (1) and the poly(A) hairpin (34). These secondary structure elements, which also should be present in single-strand sense DNA, might cause HIV-1 RT to pause and increase the

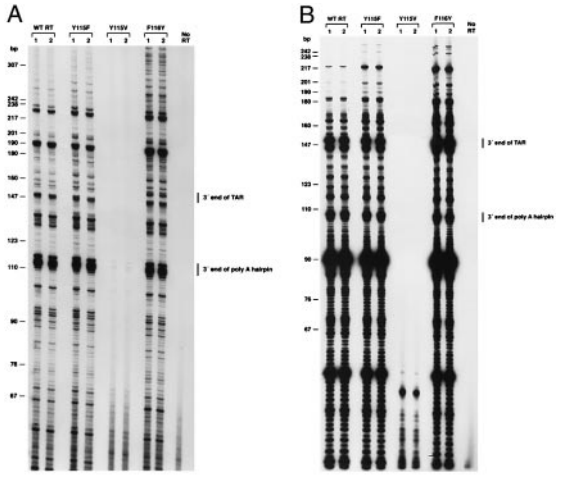

Fig. 2. Processivity assays with DNA and RNA templates. End-labeled primers were annealed to template DNA and RNA and extended in the presence of a cold trap that prevents multiple rounds of polymerization. (*A*) Processivity with the PBS DNA oligonucleotide annealed to sense PPT-PBS DNA. (*B*) Processivity with the PBS DNA oligonucleotide annealed to sense PPT-PBS RNA. The locations of the 3′ ends of two known secondary-structural elements, TAR (for a review, see ref. 1) and the poly(A) hairpin (34), are shown at the right. Duplicate assays, labeled 1 and 2, were done for each sample. WT, wild type.

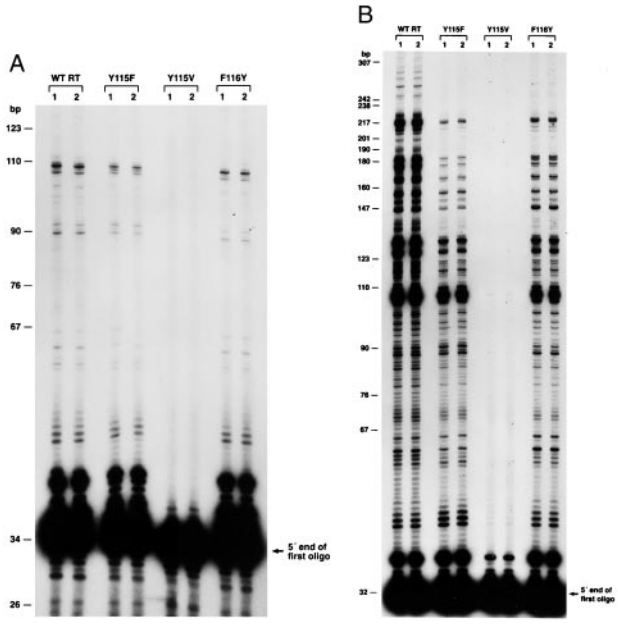

Fig. 3. Strand-displacement activity of wild-type (WT) and mutant HIV-1 RTs. The PBS DNA oligonucleotide was end-labeled with [γ^{32}P]ATP and annealed to sense single-strand DNA. A 10-fold excess of unlabeled DNA oligonucleotides also was annealed to the sense-strand DNA to provide the targets to be displaced. The RT polymerization reaction was done in the presence of two different concentrations of KCl: 75 mM KCl (*A*) and 35 mM KCl (*B*). The 5′ end of the first unlabeled target DNA oligonucleotide (marked at the right) indicates the starting point for strand displacement. Duplicate assays, labeled 1 and 2, were done for each sample.

probability of disassociation from the template primer. As shown in Fig. 2*A*, there are a series of extension products whose length corresponds to the 3′ end of the poly(A) hairpin, which is the element that the extending polymerase encounters first. There are some extension products that appear to terminate near the 3′ end of the TAR element; however, there are fewer of these products than those that correspond to the 3′ end of the poly(A) hairpin (Fig. 2*A*). Similar results were obtained when the processivity substrate was a DNA oligonucleotide annealed to single-strand M13mp18 DNA (data not shown). With a PPT oligonucleotide and an antisense HIV-1 DNA substrate, both Tyr-115–Phe and Phe-116–Tyr appeared to be slightly more processive and Tyr-115–Val was significantly less processive (data not shown).

The reported K_m for Tyr-115–Val for dTTP (62.7 μM) is significantly higher than wild-type RT (6.7 M), whereas Tyr-115–Phe has a reported K_m for dTTP of 3.0 μM (12). Although a dTTP concentration of 10 μM, which normally is used in the processivity assay, should be sufficient for wild-type RT, this concentration might be limiting for Tyr-115–Val because dTTP is present at a concentration approximately one-sixth of the reported K_m value. Therefore, we repeated the processivity assay by using a DNA oligonucleotide annealed to single-strand M13mp18 DNA but with the concentration of each nucleotide at 50 μM. The processivity for wild-type RT, Tyr-115–Phe, and Tyr-115–Val was not significantly different when the dNTP concentrations were 50 μM compared with the results with 10 μM concentrations (data not shown).

We also analyzed the processivity of the variant RTs on an RNA template. A DNA PBS oligonucleotide was hybridized to sense HIV-1 RNA (26). Again, Tyr-115–Phe and Phe-116–Tyr appear to have slightly higher processivity than the wild-type RT (Fig. 2*B*). Tyr-115–Val was significantly impaired compared with wild-type RT and the other RT variants. As described above, the sense RNA template would contain the TAR (1) and poly(A) hairpin (34) secondary structures. Interestingly, the RT extension products were somewhat different with RNA and DNA templates. As shown in Fig. 2*B*, the extension products corresponding to the 3′ end of the poly(A) hairpin, the region the RT encounters first, were not as intense with an RNA template as with a DNA template (Fig. 2*A*). The region of strongest pausing actually occurred before the poly(A) hairpin was reached (Fig. 2*A*) and there appeared to be more pausing at the 3′ end of the TAR element than with a single-strand sense DNA template.

Strand Displacement. We analyzed the strand-displacement activity of RT in the presence of both 75 mM KCl and 35 mM KCl, because Fuentes *et al.* (29) showed that 75 mM KCl (the concentration typically used in various RT assays) can inhibit strand displacement, presumably by stabilizing the nucleic acid duplex. They also showed that decreasing the concentration of KCl in the reaction increases the amount of strand displacement (14). As shown in Fig. 3*A*, 75 mM KCl inhibited strand-displacement activity by RT. Most of the PBS primers were extended only to the 5′ end of the first unlabeled oligonucleotide. The small amount of strand displacement by wild-type RT, Tyr-115–Phe, and Phe-116–Tyr extended no farther than 100 nt from the 5′ end of the first unlabeled DNA oligonucleotide. Tyr-115–Val did not appear to displace the DNA oligonucleotides to any measurable extent (Fig. 3*A*). In contrast, strand displacement was significantly increased in the presence of 35 mM KCl (Fig. 3*B*); wild-type RT extended the labeled PBS DNA oligonucleotide at least 200 nt into the double-strand substrate. Tyr-115–Phe and Phe-116–Tyr had significant levels of strand-displacement activity but did not appear to be as efficient as wild-type RT (Fig. 3*B*). Tyr-115–Val showed only a very low level of strand displacement activity even with the lower concentration of KCl.

Ribonucleotide Misincorporation. Gao *et al.* (21, 22) showed that the amino acid substitution Phe-155–Val in the MMLV RT allows the misincorporation of ribonucleotides into the growing primer strand. We tested whether mutants of HIV-1 RT with substitutions at Tyr-115, which is the amino acid equivalent to Phe-155 in the MMLV RT (30–32), would cause a similar misincorporation of ribonucleotides with a DNA:DNA template primer. Because

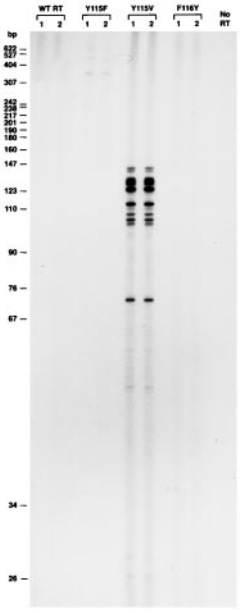

Fig. 4. UTP misincorporation by wild-type (WT) and mutant HIV-1 RTs. An unlabeled sequencing primer was annealed to single-strand M13mp18 DNA. RT polymerization was done with radioactive [α^{32}P]UTP in the reaction mixture. Extension products with UTP incorporation were radioactively labeled and visible on x-ray film. Duplicate assays, labeled 1 and 2, were done for each sample.

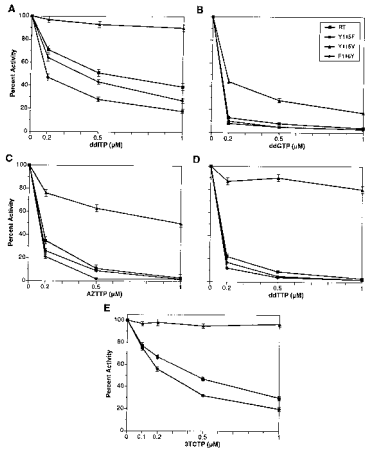

Fig. 5. Inhibition curves for various nucleoside analogs. The amount of radioactivity incorporated into the template-primer by wild-type and mutant HIV-1 RTs in the absence of inhibitor represents 100% enzyme activity. The amount of radioactivity incorporated at the various concentration of inhibitor is normalized to this value. The template primer for testing ddITP and ddGTP inhibition was poly(rC)·oligo(dG), whereas that for ddTTP and AZTTP was poly(rA)·oligo(dT). The template-primer for testing (−)-β-L-2′,3′-dideoxy-3′-thiacytidine triphosphate (3TCTP) inhibition was a sequencing primer annealed to single-strand M13mp18 DNA. When single-strand M13mp18 was used as a template with the −47 primer, the Tyr-115–Val mutant produced 36% as much DNA product as wild-type HIV-1 RT; with poly(rA)·oligo(dT) and poly(rC)·oligo(dT), the Tyr-115–Val mutant produced 50–75% as much DNA product.

[α^{32}P]UTP was the only radioactive nucleotide in this assay, any UTP that was misincorporated would label the primer strand. Note that the concentrations of dTTP and UTP (1.0 μM) were equivalent in this reaction. As shown in Fig. 4, wild-type RT and Phe-116–Tyr did not produce labeled extension products. The level of UTP misincorporation, if any, was below the limit of detection in this assay. Tyr-115–Val had a high level of UTP misincorporation, producing labeled extension products ranging between 67 and 147 nt in length (Fig. 4). This result suggests that the Tyr-115–Val RT variant was able to continue extending the primer after misincorporation of the UTP. Surprisingly, Tyr-115–Phe also appeared to misincorporate UTP into the growing primer strand, albeit at a much lower level than Tyr-115–Val (Fig. 4). We repeated these experiments using [α^{32}P]ATP as the labeled ribonucleotide. Again, Tyr-115–Val incorporated the labeled ribonucleotide to a significant extent (data not shown). However, Tyr-115–Phe did not incorporate detectable amounts of ATP.

Kinetics of Ribonucleotide Incorporation. Using kinetic assays, we analyzed the ability of wild-type RT and Tyr-115–Val to use deoxynucleotides and ribonucleotides. Wild-type RT showed a V_{max} with dGTP of 38.8 ± 0.9 pmol incorporated/min and a K_m of 4.50 ± 0.2 μM, which is similar to our previous results (26, 28). In contrast to wild-type RT, Tyr-115–Val had a slightly lower V_{max} (28.1 ± 0.4 pmol incorporated/min) and a higher K_m (8.61 ± 0.3 μM) with dGTP (data not shown). The combination of a lower V_{max} and a higher K_m might explain why Tyr-115–Val is less processive than wild-type RT (Fig. 2*A*).

There were distinct differences between wild-type RT and Tyr-115–Val when GTP was the substrate. Wild-type RT had a somewhat higher V_{max} than did Tyr-115–Val (0.17 ± 0.01 pmol GTP incorporated/min versus 0.10 ± 0.03 pmol GTP incorporated/min); the V_{max} for either enzyme was much lower for GTP than dGTP. There was a larger difference in the K_m. Wild-type RT had a K_m of 23.1 ± 0.10 μM GTP; Tyr-115–Val had a K_m of 1.47 ± 0.12 μM GTP (data not shown).

Nucleoside Analog Resistance. Because Tyr-115–Val showed a decreased ability to discriminate between deoxyribose and ribose, we wanted to determine whether Tyr-115–Val could discriminate between normal dNTPs and various nucleoside analogs. We tested three dideoxyribonucleotide analogs as well as AZTTP and (−)-β-L-2′,3′-dideoxy-3′-thiacytidine triphosphate (3TLTP). As shown in Fig. 5, Tyr-115–Val was less sensitive to all of the nucleoside analogs than was wild-type RT. Tyr-115–Phe and Phe-116–Tyr appeared to be slightly more sensitive to the compounds than wild-type RT (Fig. 6). Tisdale *et al.* (16) showed that a virus containing the Tyr-115–Phe mutation is as susceptible as wild-type RT to several different nucleoside analogs. The exception is the carbocyclic nucleoside analog 1592U89; the resistance of the Tyr-115–Phe variant was about twice that of wild-type RT for this analog (16).

Discussion

Although the fidelity of HIV-1 RT is lower than that of some DNA polymerases, RT does select the proper dNTP to be added to the primer strand with considerable accuracy (approximately 1 error for every 10^4 bases polymerized) (see ref. 1 for a review). A dTTP residue has been modeled into the structure of HIV-1 RT in complex with double-strand DNA (5). A model for the structure of binding of a nucleoside triphosphate to MMLV RT also has been developed (31). Both models propose that the equivalent amino acids in the two structures (Tyr-115 in HIV-1 RT, Phe-155 in MMLV RT) interact with the ribose of the incoming triphosphate. The structure of a ternary complex of HIV-1 RT, double-strand DNA, and a bound dTTP (6) confirms these predictions and provides a more precise picture of the actual interactions of the protein and the triphosphate at the active site (Fig. 6). To explore the consequences of altering amino acids in the nucleotide binding pocket, we have analyzed the effects of the amino acid substitutions Tyr-115–Phe, Tyr-115–Val, and Phe-116–Tyr.

The effects of an amino acid substitution on HIV-1 RT can be subtle and may not be easily detected by using a simple polymerase assay with a homopolymeric template primer such as

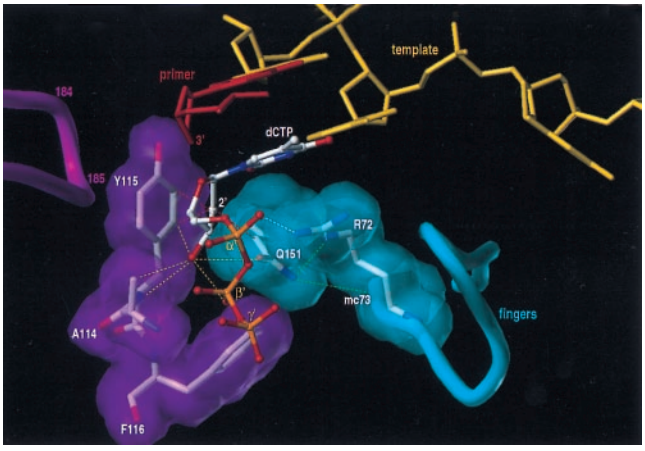

Fig. 6. View of the polymerase active site of HIV-1 RT. The sugar ring of the incoming dCTP is positioned between the hydrophobic side chains of Tyr-115 and Ala-114 at the back (Van der Waals spheres in purple), and Glu-151 and Arg-72 in front (Van der Waals spheres in cyan). Phe-116, although too far away to interact directly with the sugar of the dCTP, forms the floor of the 3′ OH binding pocket (Van der Waals spheres in purple). Yellow lines indicate interactions of the 3′ OH of dCTP with the ring of Tyr-115, the main-chain NH of Tyr-115, the main-chain NH of Ala-114, β-phosphate of dCTP, and CO of Glu-151. Bridging interactions of the NH group of Glu-151 with the guanidinium of Arg-72 and the main-chain CO of Lys-73 are shown as green dotted lines. The interactions of the Tyr-115 ring and the Glu-151 side chain with the 2′ carbon of dCTP are shown as red dotted lines.

poly(rC)·oligo(dG). Using HIV-1 genome-based templates, Tyr-115–Phe is similar to wild-type RT in the RDDP, DDDP, and processivity assays (Figs. 1 *A* and *B* and 2 *A* and *B*). However, it is clear in the strand displacement assay that the RT variant Tyr-115–Phe is impaired relative to the wild-type enzyme (Fig. 3). As will be discussed below, Tyr-115–Phe also might have a decreased ability to select dNTPs over NTPs. In contrast, the RT variant Phe-116–Tyr appears to be better than wild-type RT in most of the RDDP and DDDP assays (Fig. 1 *A* and *B*) and is more processive than wild-type RT (Fig. 2*A* and *B*). However, this variant also is impaired in the strand displacement assay relative to wild-type RT (Fig. 3*A*).

The effects of Tyr-115–Val amino acid substitution are not subtle, however. With the exception of the template primer poly(rC)·oligo(dG), this enzyme is significantly impaired in both the RDDP and DDDP assays compared with wild-type RT (Fig. 1 *A* and *B*). The Tyr-115–Val variant is also significantly less processive than wild-type RT with a variety of template-primers (Fig. 2 *A* and *B*). Tyr-115–Val has been reported to have a much higher K_m for dTTP (62.7 μM) than does wild-type RT (6.7 μM) (12). We found that Tyr-115–Val has a higher K_m for dGTP than does wild-type RT (8.61 μM dGTP versus 4.50 μM) and a lower V_{max} (28.1 pmol dGTP incorporated/min versus 38.8 pmol incorporated/min for wild-type RT). However, the K_m we measured for dGTP is significantly lower than the reported value for dTTP. Taken together, the available data suggest not only that the Tyr-115–Val RT variant binds the incoming dNTP more weakly than wild-type RT but that it binds the incoming dNTP improperly: the difference in the V_{max} shows that increasing the concentration of dNTPs did not completely compensate for the improper binding of the dNTP.

Mispositioning of the incoming nucleotide also might allow the RT variant Tyr-115–Val to incorporate NTPs (Fig. 4). The equivalent Phe-155–Val mutation in MMLV RT causes a loss of discrimination between dNTPs and NTPs rather than a complete switch of substrate specificity (21, 33). Wild-type MMLV RT has a K_m for UTP that is much higher than the K_m for dTTP (443 μM versus 9.2 μM). There is a similar effect on V_{max}. Both wild-type MMLV RT and the Phe-155–Val mutant have similar V_{max} values for dTTP (0.38 and 0.41 μmol/min per mg, respectively). The rate for dTTP incorporation is much higher than for UTP (1.17 versus 5.45 μmol/min per mg). For the Phe-155–Val variant, the K_m values are similar (4.34 μM versus 13.7 μM for the wild-type RT) (21). Our data suggest that the Tyr-115–Val variant of HIV-1 RT also has lost substrate specificity. However, there are important differences between the results obtained with the Phe-155–Val MMLV RT variant and those obtained with the Tyr-115–Val HIV-1 RT variant. As described above, Tyr-115–Val has been reported to have a significantly higher K_m for dTTP (62.7 μM) than wild-type HIV-1 RT (6.7 μM) (12). The difference in the dTTP K_m values between wild-type MMLV RT and the MMLV RT variant is much smaller (21).

We measured the K_m and V_{max} values for wild-type HIV-1 RT and the Tyr-115–Val variant with both dGTP and GTP. In contrast to wild-type MMLV RT, wild-type HIV-1 RT did not have a large difference in the K_m values between dGTP and GTP. The K_m for dGTP was 4.50 μM whereas the K_m for GTP was 23.1 μM. The most significant difference was in the V_{max} for wild-type RT, which was 38.8 pmol incorporated/min for dGTP versus only 0.17 pmol incorporated/min for GTP (data not shown). This result suggests that wild-type HIV-1 RT can bind GTP, but does so in a fashion that is unfavorable for polymerization. Interestingly, Tyr-115–Val had a somewhat lower V_{max} with GTP than did wild-type RT (data not shown), yet in the UTP misincorporation assay, Tyr-115–Val clearly incorporated UTP into the extended primer whereas no incorporation was detected for wild-type HIV-1 RT (Fig. 4).

The answer to this apparent paradox might be found in the K_m values. The Tyr-115–Val mutant had a low K_m value (1.47 μM), whereas the wild-type RT had a significantly higher K_m (23.1 μM). The level of [α^{32}P]UTP in the UTP misincorporation assay was low (1 μM) and was equal to the level of the preferred substrate (1 μM dTTP). If Tyr-115–Val also had a lower K_m for UTP relative to wild-type RT, the results of the UTP misincorporation might reflect an ability of Tyr-115–Val to bind NTPs at the polymerase active site better than wild-type RT, rather than an increase in the ability to (mis)incorporate NTPs.

It has been proposed that the presence of a phenyl ring at residue 155 of MMLV RT acts directly as a steric gate that distinguishes between a 2′ H group of a dNTP and a 2′ OH group of an NTP (22, 28, 31). In this model, the Phe-155–Val mutant replaces the bulky aromatic side chain with the smaller side group of valine and removes the steric gate. The structure of a ternary complex of HIV-1 RT, double-strand DNA, and a dTTP (Fig. 6), although different from the proposed model in structural detail, suggests that the corresponding amino acid Tyr-115 plays a role in forming a steric gate in concert with Q151 (5). As shown in Fig. 6, the 2′ and 3′ positions of the incoming dNTP are flanked on one side by the Tyr-115 aromatic side chain and on the other side by the Q151 side chain. The 2′ position of the dNTP is closer to the aliphatic side chain and the main-chain carbonyl oxygen of Q151 (3.4 and 3.0 Å) than to the side chain of Tyr-115 (3.5 Å). Nevertheless, the sugar puckering of the dNTP directs a 2′ OH to the ring of Tyr-115 rather than to the Q151 side chain. In the Tyr-115Val mutant, the aromatic side chain is replaced by a shorter, more rigid, branched residue. This side chain would be expected to move toward the dNTP binding site because of unfavorable interactions with the main-chain carbonyl oxygen of residue 149, a movement that should permit the introduction of an OH group at the 2′ sugar position.

Although the mutant Tyr-115–Val was able to incorporate UTP, ATP, and GTP more efficiently than wild-type RT, the other properties of Tyr-115–Val suggest that the amino acid at position 115 has additional roles beyond that of participating in a simple steric gate. Tyr-115–Val was clearly defective compared with wild-type HIV-1 RT in most of our assays. This mutant had a much lower processivity activity with both RNA and DNA templates than did wild-type RT, and it was unable to cause strand displacement under any of the conditions we tested. However, Tyr-115–Val RT showed

a high degree of resistance to all of the nucleoside analogs that we tested. In the absence of a three-dimensional structure of the Tyr-115–Val RT variant with a bound nucleotide, it is unclear how the variant is able to select the proper dNTP over a nucleoside analog more effectively than wild-type HIV-1 RT. However, if the Tyr-115–Val variant inappropriately positions the incoming dNTP, it also might bind the nucleoside analog incorrectly, suggesting that there are steric constraints that help the mutant enzyme discriminate against certain modified sugars. Although the degree of resistance to nucleoside analogs is significant, the Tyr-115–Val mutation has not been found in HIV-1 patients treated with nucleoside analogs. This is presumably a result of the fact that mutations like Tyr-115–Val cause sufficient distortion of the polymerase active site such that HIV-1 variants carrying these mutations cannot be selected. In support of this idea, an MMLV RT variant with an Phe-155–Val mutation does not replicate (22).

Tyr-115–Val is more efficient at extending a mismatched base pair than is wild-type HIV RT (12). It should be remembered that this assay does not directly measure the fidelity; rather, it measures how well the variants can incorporate dNTPs with a less-than-optimal template primer configuration at the active site. The incoming dNTP can be considered to have two components: a base and a ribose phosphate. The overall fidelity of the enzyme depends primarily on how well the base of the incoming dNTP is matched to the complementary base on the template strand. The mispair extension assay primarily involves the ribose phosphate and how well the enzyme can add an incoming dNTP to the mispaired base at the 3′ end of the primer strand. As discussed above, the Tyr-115–Val variant may improperly position the incoming dNTP. This mispositioning of the dNTP might allow the Tyr-115–Val variant to extend a mismatched pair more efficiently than wild-type HIV-1 RT, but this result does not necessarily mean the enzyme has a lower fidelity than the wild-type enzyme. Although the ability to extend a primer to which the wrong base already has been added is a component of fidelity, this event is secondary to the misincorporation of a dNTP.

It has been suggested that an MMLV containing the Phe-155–Val mutation in the RT coding region is defective in its replication because ribonucleotides, once incorporated into the growing DNA strand, act as inhibitors of DNA synthesis (22). However, the incorporation of ribonucleotides does not appear to block DNA synthesis by the HIV-1 RT variants Tyr-115–Phe and Tyr-115–Val (Fig. 4). It should be noted that the extension products for both Tyr-115–Val and Tyr-115–Phe in the UTP misincorporation assay are relatively large. The major extension products for Tyr-115–Val range in size between 67 and 147 nt, and the extension products for Tyr-115–Phe are more than 300 nt in size. This result suggests that both Tyr-115–Val and Tyr-115–Phe are able to extend the primer strand after the misincorporation of UTP.

In summary, the amino acid residue Tyr-115 of HIV-1 RT has an important role in the selection of the proper nucleotide during polymerization. Although the amino acid substitution Tyr-115–Phe has little effect on the enzyme, the mutation Tyr-115–Val has deleterious effects on polymerization. The equivalent positions in other polymerases also appear to function in the selection of the proper nucleotide and in the rejection of inappropriate substrates (for a review, see ref. 30). As more is learned about the nucleotide binding region(s) of polymerases, it may be possible to engineer polymerases with novel substrate specificities (33).

We are most grateful to Pat Clark and Peter Frank for enzyme purification, A. Arthur for expert editorial assistance, and H. Marusiodis for help in preparing this paper. The research in S.H.H.'s laboratory was sponsored by the National Cancer Institute, Department of Health and Human Services, under contract with Advanced BioScience Laboratories, and by the National Institute of General Medical Sciences. The research in E.A.'s laboratory was supported by National Institutes of Health Grants GM 56609 and AI 27690 (to E.A.) and National Institutes of Health National Research Service Award Postdoctoral Fellowship AI 09578 (to S.G.S.).

1. Coffin, J. M., Hughes, S. H. & Varmus, H. E. (1997) *Retroviruses* (Cold Spring Harbor Lab. Press, Plainview, NY).
2. De Clercq, E. (1994) *Biochem. Pharmacol.* **47,** 155–169.
3. Mellors, J. W., Larder, B. A. & Schinazi, R. G. (1995) *Int. Antiviral News* **3,** 8–13.
4. Richman, D. D. (1993) *Antimicrob. Agents Chemother.* **37,** 1207–1213.
5. Ding, J., Das, K., Hsiou, Y., Sarafianos, S. G., Clark, A. D., Jr., Jacobo-Molina, A., Tantillo, C., Hughes, S. H. & Arnold, E. (1998) *J. Mol. Biol.* **284,** 1095–1111.
6. Huang, H., Chopra, R., Verdine, G. L. & Harrison, S. C. (1998) *Science* **282,** 1669–1675.
7. Boyer, P. L., Ferris, A. L. & Hughes, S. H. (1992) *J. Virol.* **66,** 1031–1039.
8. Boyer, P. L., Ferris, A. L., Clark, P., Whitmer, J., Frank, P., Tantillo, C., Arnold, E. & Hughes, S. H. (1994) *J. Mol. Biol.* **243,** 472–483.
9. Larder, B. A., Kemp, S. D. & Purifoy, D. J. M. (1989) *Proc. Natl. Acad. Sci. USA* **86,** 4803–4807.
10. Lowe, D. M., Parmar, V., Kemp. S. D. & Larder, B. A. (1991) *FEBS Lett.* **282,** 231–234.
11. Martín-Hernández, A., Domingo, E. & Menèndez-Arias, L. (1996) *EMBO J.* **15,** 4434–4442.
12. Martín-Hernández, A. M., Gutièrrez-Rivas, M., Domingo, E. & Menèndez-Arias, L. (1997) *Nucleic Acids Res.* **25,** 1383–1389.
13. Wrobel, J. A., Chao, S.-F., Conrad, M. J., Merker, J. D., Swanstrom, R., Pielak, G. J. & Hutchison, C. A., III (1998) *Proc. Natl. Acad. Sci. USA* **95,** 638–645.
14. Harris, D., Kaushik, N., Pandey, P. K., Yadav, P. N. S. & Pandey, V. N. (1998) *J. Biol. Chem.* **273,** 33624–33634.
15. Vandamme, A.-M., Van Vaerenbergh, K. & De Clercq, E. (1998) *Antiviral Chem. Chemother.* **9,** 187–203.
16. Tisdale, M., Alnadaf, T. & Cousens, D. (1997) *Antimicrob. Agents Chemother.* **41,** 1094–1098.
17. Rezende, L. F., Curr, K., Ueno, T., Mitsuya, H. & Prasad, V. R. (1998) *J. Virol.* **72,** 2890–2895.
18. Schafer, R. W., Kozal, M. J., Winters, M. A., Iverson, A. K. N., Katzenstein, D. A., Ragni, M. V., Meyer, W. A., III, Gupta, P., Rasheed, S., Coombs, R., *et al*. (1994) *J. Infect. Dis.* **169,** 722–729.
19. Shirasaka, T., Kavlick, M. F., Ueno, T., Gao, W.-Y., Kojima, E., Alcaide, M. L., Chokekijchai, S., Roy, B. M., Arnold, E., Yarchoan, R. & Mitsuya, H. (1995) *Proc. Natl. Acad. Sci. USA* **92,** 2398–2402.
20. Poch, O., Sauvaget, I., Delarue, M. & Tordo, N. (1989) *EMBO J.* **8,** 3867–3874.
21. Gao, G., Orlova, M., Georgiadis, M. M., Hendrickson, W. A. & Goff, S. P. (1997) *Proc. Natl. Acad. Sci. USA* **94,** 407–411.
22. Gao, G. & Goff, S. P. (1998) *J. Virol.* **72,** 5905–5911.
23. Boyer, P. L., Ferris, A. L. & Hughes, S. H. (1992) *J. Virol.* **66,** 7533–7537.
24. Boyer, P. L., Tantillo, C., Jacobo-Molina, A., Nanni, R. G., Ding, J., Arnold, E. & Hughes, S. H. (1994) *Proc. Natl. Acad. Sci. USA* **91,** 4882–4886.
25. Adachi, A., Gendelman, H. E., Koenig, S., Folks, T., Wiley, R. A., Rabson, A. & Martin, M. A. (1986) *J. Virol.* **59,** 284–291.
26. Boyer, P. L., Liszienicz, J., Lori, F. & Hughes, S. H. (1999) *J. Mol. Biol.* **286,** 995–1008.
27. Boyer, P. L. & Hughes, S. H. (1995) *Antimicrob. Agents Chemother.* **39,** 1624–1628.
28. Boyer, P. L., Gao, H.-Q. & Hughes, S. H. (1998) *Antimicrob. Agents Chemother.* **42,** 447–452.
29. Fuentes, G. M., Rodríguez, L., Palaniappan, C., Fay, P. J. & Bambara, R. A. (1996) *J. Biol. Chem.* **271,** 1966–1971.
30. Barber, A., Hizi, A., Maizel, J. V., Jr. & Hughes, S. H. (1990) *AIDS Res. Human Retrovir.* **6,** 1061–1072.
31. Georgiadis, M. M., Jessen, S. M., Ogata, C. M., Telesnitsky, A., Goff, S. P. & Hendrickson, W. A. (1995) *Structure (London)* **3,** 879–892.
32. Johnson, M. S., McClure, M. A., Feng, D. F., Gray, J. & Doolittle, R. (1986) *Proc. Natl. Acad. Sci. USA* **83,** 7648–7652.
33. Joyce, C. M. (1997) *Proc. Natl. Acad. Sci. USA* **94,** 1619–1622.
34. Das, A. T., Klaver, B., Klasens, B. I. F., van Wamel, J. L. B. & Berkhout, B. (1997) *J. Virol.* **71,** 2346–2356.